# DESIGN AND TEST RESULTS ON A 45-KV PULSED POWER MODULATOR FOR A 1.5-MW MAGNETRON APPLICATION OF KSTAR LHCD

SUNG-DUCK JANG*, YOON-GYU SON, JONG-SEOK OH, YOUNG-SOON BAE[1], MOO-HYUN CHO and WON NAMKUNG
Division of Engineering, Pohang Accelerator Laboratory, Pohang University of Science and Technology
San 31, Hyoja-dong, Nam-Gu, Pohang, Kyungbuk, 790-784, Korea
[1]National Fusion Research Center, Daejeon 305-333
*Corresponding author. E-mail : sdjang@postech.ac.kr

*Received January 26, 2006*
*Accepted for Publication October 21, 2006*

The microwave heating system of KSTAR consists of ECH and LHCD. ECH and LHCD offer the benefits of a reliable operation at the start of plasma formation and a non-inductive current drive durable steady state operation, respectively. LHCD uses a C-band microwave system with a frequency of 5 GHz. A pulsed power modulator with a power of 3.6 MW, 4 μS, 200 pps is required to drive the high-powered magnetron. The development of a pulse modulator with 1:4 pulse transformers is the focus of the research in this study. The peak power handling capability is 3.6 MW (45 kV, 90 A at load side with a pulse width of 4 μS). This paper describes the system overview and test results of the pulsed modulator. In particular, a simulated waveform is compared with the tested waveform.

**KEYWORDS** : KSTAR LHCD, Pulsed Power Modulator, Pulse Transformer

## 1. INTRODUCTION

The microwave heating system of KSTAR consists of ECH and LHCD. LHCD uses a C-band microwave system with a frequency of 5 GHz. The KSTAR LHCD system is presently under design for the steady-state operation of KSTAR [1]. The steady-state operation of the KSTAR requires an appropriate LH launcher design capable of sustaining the high thermal heat load from the plasma. The LH launcher design is also under design in collaboration with Princeton Plasma Physics Laboratory (PPPL) in the US.

The launcher is composed primarily of numerous waveguide channels milled with a waveguide pattern of a 3-dB power splitter, fixed phase shifter, and H-plane taper with the grill facing the plasma [2]. The basic design of this waveguide channel and grill has been completed, and a test model of the 3-dB power splitter, which is the principal element of the channel, has been fabricated in a realistic scale. A low-power RF test of the test model was in good agreement with the design value [3]. A breakdown of the 3-dB power splitter is planned, as is power splitting for CW (Continuous Wave) high-power operations with an RF power density of 3.7 kW/cm$^2$ in the channel. For this test, 5-GHz 10-kW CW high-power RF system is needed. However, in that a 5-GHz RF source generating 10-kW CW is currently unavailable, a pulsed high-power RF system has been manufactured using a 5-GHz 1.5-MW magnetron instead. The 5-GHz magnetron was purchased from Communication Power Industries (CPI). The peak output power and the pulse length of the CPI magnetron (model SFD-369) is 1.6-MW and 1 μS, respectively. A pulse modulator with a power of 3.6 MW, 4 μS, and 200 pps (pulse per second) is required to drive the CPI magnetron. The modulator system relies on pulse transformer to step the peak pulse voltage up to 45 kV. The high-power pulse transformer has the function of transferring the pulse energy from a pulsed power source to a high-power load. The pulse transformer produces a pulse with a peak voltage of 45 kV which is required to produce a 5-GHz microwave source in a 1.5-MW magnetron. The peak power handling capability is 3.6-MW (45 kV, 90 A at the load side with a 4 μS pulse width). A high-power pulse transformer for a magnetron was studied in a previous paper [4]. The present paper shows an overview of the pulsed 5 GHz RF system design in addition to test results of the pulsed modulator focused on an analysis of an equivalent circuit and parameters of the high-power pulse transformer. Particular attention is paid to a comparison of the simulated waveform with the tested waveform.

## 2. DESIGN CONSIDERATIONS

A pulse transformer and its associated pulse generator and load can be represented by an equivalent circuit. Fig. 1 shows a simplified equivalent circuit of a pulse generator, step-up pulse transformer and load [5] [6].

By analyzing the behavior of each of equivalent circuit for a given pulse width ($\tau$) and load ($R_L$, $C_L$), transformer parameters such as the primary inductance ($L_p$), leakage inductance ($L_L$) and distributed capacitance ($C_D$) can be determined and thereby optimized for the best pulse response.

These transformer parameters are a function of the coil geometry and winding configuration, the dielectric constant of the insulation, and the permeability of the core material. Fig. 2 shows the coil geometry and winding configuration of the pulse transformer.

Transformer parameters such as the shunt inductance ($L_p$), leakage inductance ($L_L$) and distributed capacitance ($C_D$) are given by Eqs. (1), (2), (3), respectively [5]. The best design is the one with the lowest LC product, provided that it has the proper matching L-C ratio.

$$L_L \cong 2\pi(a+b+4\Delta_{12})N_s^2\left(\frac{\Delta_{12}}{l_c}\right) \quad [\text{nH}] \tag{1}$$

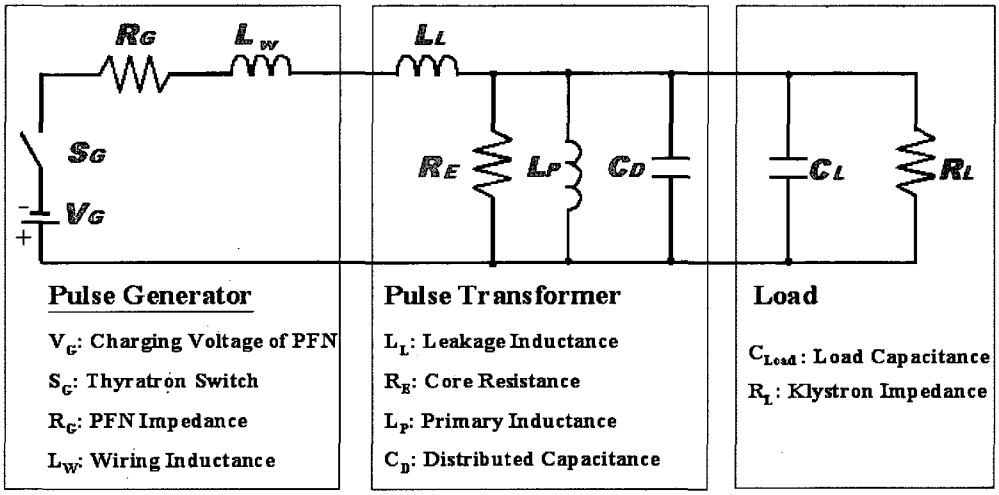


Fig. 1. Simplified Equivalent Circuit of a Pulse Modulator System

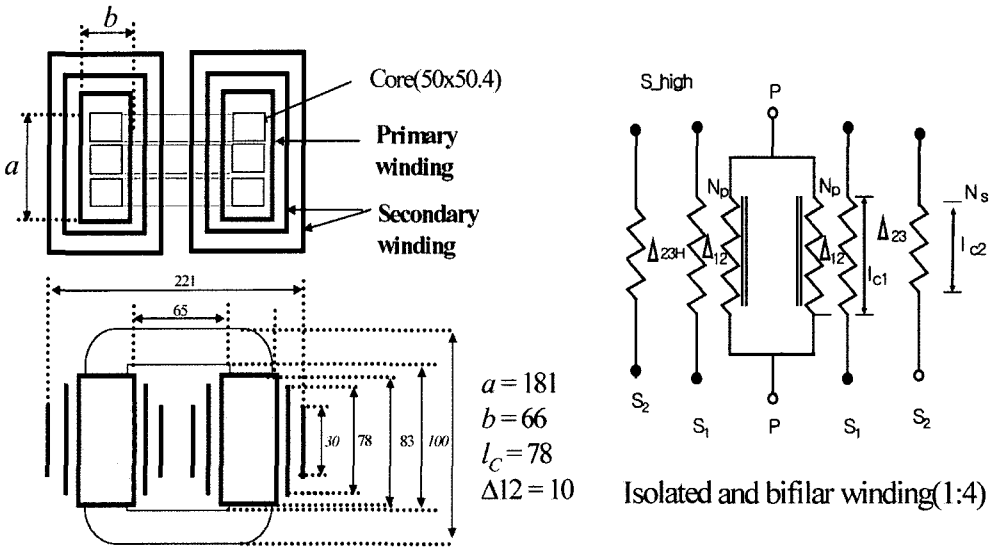


Fig. 2. Coil Geometry and Winding Configuration

$$C_D \cong \frac{1}{2}\left(\frac{8.854\varepsilon_r U_c l_c}{\Delta_{12}}\right)\left(\frac{n-1}{n}\right)^2 \quad [\text{pF}] \qquad (2)$$

$$L_p \cong 4\pi\mu_e N_p^{\,2}\frac{A_m}{l_m} \quad [\text{nH}] \qquad (3)$$

In the equations, $N_p$ is the number of turns in the primary coil, $N_s$ is the number of turns in the secondary coil, $\triangle$ represents the insulation distance between layers, $U_c$ denotes the average circumference of the layers between the primary and secondary windings in cm, $l_c$ is the winding length in cm, $\varepsilon_r$ is the relative dielectric constant of the insulating material between the layers, $\mu_e$ is the relative pulse permeability of the core, $A_m$ is the cross-sectional area of the core, $l_m$ is the mean magnetic path length of the core, and n is the step-up ratio.

## 2.1 Rise Time Analysis

The pulse efficiency depends on detailed design parameters of the pulsing system, including a pulse transformer and a load. The rise time is related to high-frequency components due to the high-impedance characteristics of these components. It is possible to neglect the effect of the shunt resistance $R_e$ and the shunt inductance $L_P$ during the short rise time in a leading-edge analysis.

The normalized load voltage y(t) defined as

$$y(t)=\frac{V_L(t)}{V_G}\left(\frac{1+m}{m}\right) \qquad (4)$$

is given by

$$y(t)=\left\{1-e^{-at}\left(\frac{a}{w}\sin wt+\cos wt\right)\right\} \quad (\sigma<1) \qquad (5)$$

$$y(t)=\left\{1-e^{-at}\left(\frac{a}{k}\sinh kt+\cosh kt\right)\right\} \quad (\sigma\geq 1) \qquad (6)$$

where $a=\frac{2\pi\sigma}{\tau}$, $k=\frac{2\pi\sqrt{\sigma^2-1}}{\tau}$, $w=\frac{2\pi\sqrt{1-\sigma^2}}{\tau}$,

$$\sigma=\frac{1}{2\pi\sqrt{m(m+1)}}\left(\gamma m+\frac{1}{\gamma}\right), \tau=2\pi\sqrt{\frac{m}{(m+1)}}\sqrt{L_T C_T},$$

$$m=\frac{R_L}{R_G},\ \gamma=\frac{Z_T}{R_L},\ Z_T=\sqrt{\frac{L_T}{C_T}}$$

$$L_T=L_W+L_L,\ C_T=C_D+C_L$$

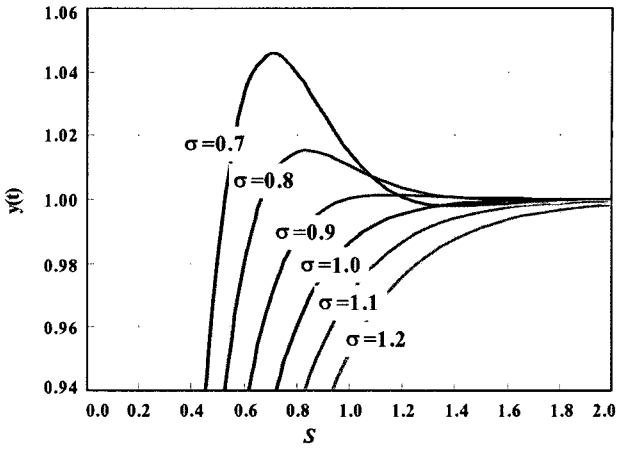


Fig. 3. Normalized Rising-pulse Waveform for Various Values of the Damping Factor

Here, m is the matching parameter between the generator and the load, and $\gamma$ is the impedance matching parameter between the transformation system and the load. $Z_T$ is the transformation impedance of the pulsing system.

An expanded view of the leading edge of y(t) near the flat top is shown in Fig. 3 as a function of the damping factor $\sigma$. In this figure, the normalized time S is defined by $S=t/\tau$. The pulse shape and the rise time are sensitive to the damping factor $\sigma$ in the front part of the pulse waveform. For given values of $L_T$ and $C_T$, a small $\sigma$ value results in a fast rise time but generates a large overshoot. For a matched load (m=1), the rise time is determined by

$$t_r=\sqrt{2}\pi S(\sigma)\sqrt{L_T C_T} \qquad (7)$$

where S ($\sigma$) is a fitting function to give the rise time from 10% to 90% of the maximum pulse height.

In general, a pulse flat-top with less than ± 0.5% ripple is required to produce the high-efficiency pulse ($T_{rf}/T_p$) which is defined by the ratio of the available flat-top width for an effective RF power, $T_{rf}$, to the given output pulse width, $T_p$. The damping factor $\sigma$ must be larger than 0.86 in order to limit the overshoot to less than 0.5% during the flat-top [7].

## 2.2 Droop and Core Size

The pulse magnetization of the core, droop, and core volume is given by (8), (9) and (10), respectively.

$$V_s\tau_w=10^{-8}\Delta B N_S A_e \qquad (8)$$

$$D_r=\frac{R_L\tau_w}{2L_s}=\frac{\Delta B R_L l_m}{2\mu_0\mu_e V_s N_s} \qquad (9)$$

$$V_{core} = \frac{2\mu_o \mu_e}{\Delta B^2} P.\tau_w.D_r \qquad (10)$$

In the equations, $\triangle B$ denotes the average increment of the magnetic flux density of the core in gauss, $A_e$ represents the effective cross-sectional area of the core, $L_s$ is the number of secondary turns, $V_s$ is the load voltage in volts, P is the power handling capability of the core, and $\tau_w$ is the pulse width.

From the above analysis, a fast rise time can be realized by reducing the number of secondary turns; however, this produces a larger pulse droop and a larger core size. Thus, a tradeoff among these parameters is required to generate the optimum output pulse [8]. The design procedure of a pulsed RF system that addresses this issue is summarized in Fig. 4.

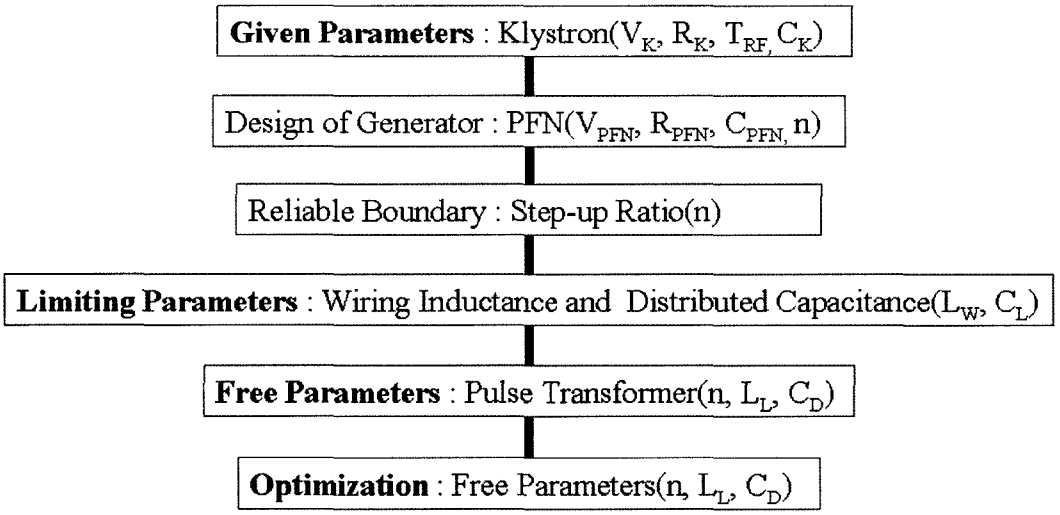


Fig. 4. Design Procedure of the Pulsed RF System

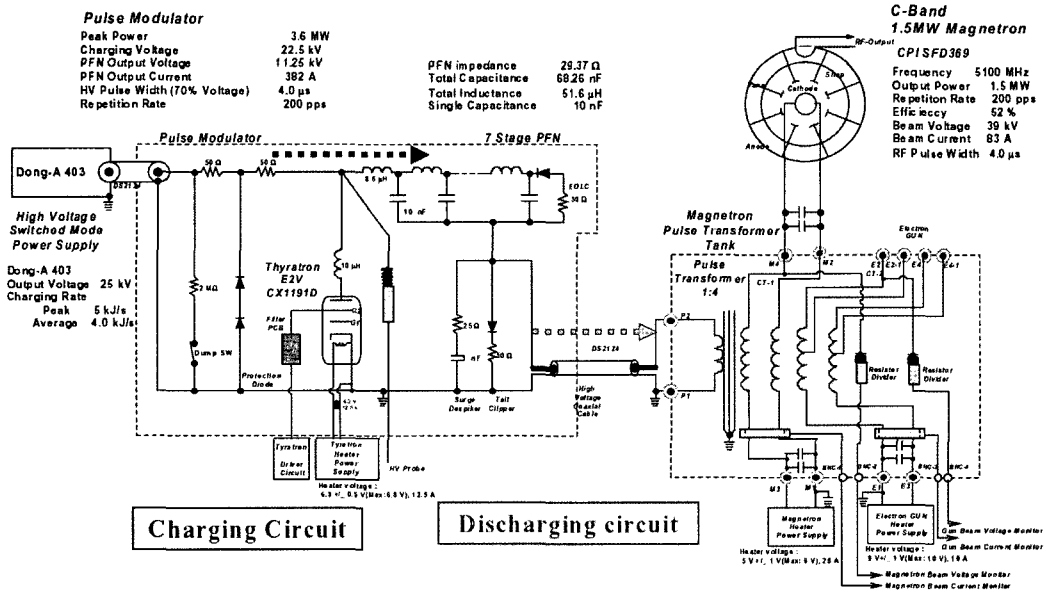


Fig. 5. Main Circuit Diagram of the Pulse Modulator for the 5-GHz Low-power Test System

## 3. SYSTEM DESCRIPTION

A line-type pulse modulator is used to drive a 1.5-MW magnetron for a LHCD low-power test system. Fig. 5 shows a main circuit diagram of the pulse modulator for a 5-GHz low-power test system [9]. The main components of this system are composed of the seven stages of the PFN, a thyratron tube switch (E2V,CX11910), and a 1:4 step-up pulse transformer.

In this system, the pulse energy is initially stored in an artificial delay-line pulse forming network (PFN). It is then periodically discharged into the primary winding of the pulse transformer by a gaseous discharge switch, or a thyratron tube. During the inter-pulse period, the PFN is recharged from a dc power supply. The pulse transformer also made it possible to match the impedance of the load to a power source for a maximum transfer of energy from the modulator to a microwave electron tube. Table 1 describes the main specifications of the pulse transformer for a 1.5-MW magnetron.

The 1:4 pulse transformers were designed and manufactured. In practice, a negative polarity pulse is applied to the magnetron's hot cathode. An isolated and secondary bifilar winding technique was used for the voltage distribution of the high-voltage pulse transformer [5,6]. A cathode heater power can be supplied to the cathode by means of a bifilar secondary winding of the pulse transformer.

Fig. 6 shows the fabricated pulse transformer. It is composed of three subcores, primary windings, secondary windings and supporting structures. Each subcore is wound from a grain-oriented silicon steel sheet (0.05 mm thickness, Microsil, "ML" cut core) manufactured by Magnetic Metals Corporation. The primary windings are made of Cu wire ($\Phi$ 1.6mm) using 10 turns for each leg of the core, and the windings are connected to the terminal in parallel. Secondary windings are made of Cu wire ($\Phi$ 1.8mm) using 40 turns, which are divided into two parts and connected to the terminal in parallel.

**Table 1**. Specifications of a Pulse Transformer

| Parameter | Value |
|---|---|
| Pulse droop [%] | 4 |
| Rising time [μS] | 0.7 |
| Step-up ratio | 4 |
| Primary voltage [kV] | 11.25 |
| Primary current [A] | 375 |
| Secondary voltage [kV] | 45 |
| Secondary current [A] | 96 |
| Load impedance [ Ω ] | 470 |
| Flat-top pulse width [μS] | 4 |
| Pulse Energy [J] | 17.3 |
| Repetition rate, max [Hz] | 200 |

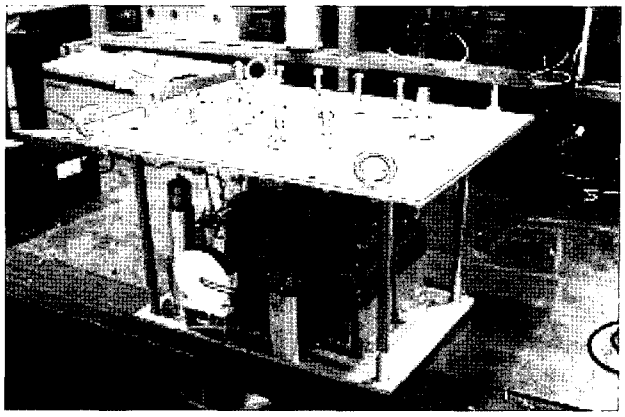

Fig. 6. Photograph of the 1:4 Pulse Transformer

## 4. DESIGN AND TEST RESULTS

### 4.1 Transformer Design Results

The effective pulse permeability is a very important parameter in the design of pulse transformers. To estimate the droop of the load voltage, information regarding the primary inductance is needed, as determined by the effective pulse permeability, core cross-section, magnetic path length and number of turns. The effective pulse permeability can be obtained using the load voltage droop. The designed effective pulse permeability of the cut core was selected as 800 based on a previous study by the authors [10]. The leakage inductance was measured by an LCR meter (Hioki 3532) connected across the primary winding with the secondary winding shorted, and also calculated by Eq. (1). The transformer parameters were measured after the transformer was assembled. The main designed and measured parameters of the secondary of the pulse transformer are summarized in Table 2.

### 4.2 High-Voltage and High-Power Test

Initially, the PFN modulator was tested with a 472 Ω resistive load to measure the transformer characteristics using a circuit layout, as shown by Fig. 4. In the system, the PFN capacitor was charged to a voltage of 25 kV by using a high-voltage inverter power supply [11]. By tuning the PFN inductance, the output voltage of the pulse transformer was set to the desired rise-time and flat-topped pulse.

**Table 2.** Main Parameters of the Pulse Transformer

| Parameters | Designed | Measured |
|---|---|---|
| Turns ratio | 1:4 | 1:4 |
| Primary turns | 10 | 10 |
| Leakage inductance | 37 μH | 42.2 μH |
| Distributed capacitance | 12.82 pF | 38.78 pF |
| Primary inductance | 21.6 mH | 19.85 mH |
| Magnetic flux swing | 0.68 T | - |
| Effective permeability | 800 | - |
| Gap length | 24 ㎛ | 24 ㎛ |
| Effective core cross-section | 66 ㎠ | - |
| Mean magnetic path length | 50.3 ㎝ | - |
| Core weight | 47 ㎏ | - |

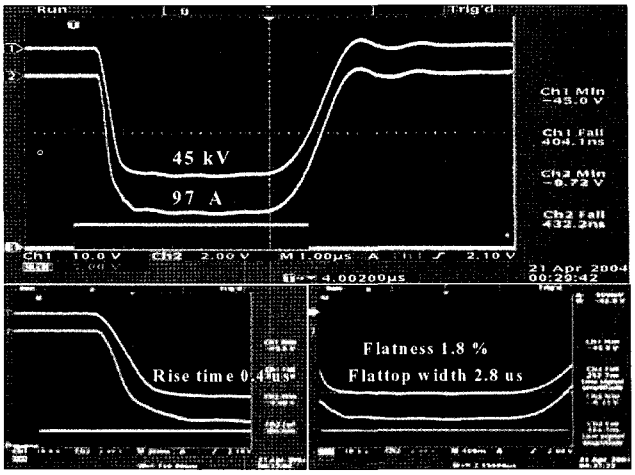


Fig. 7. Load Voltage and Current Waveform with the 472 Ω Resistor (Ch. 2 (1000X), Ch. 2 (10X))

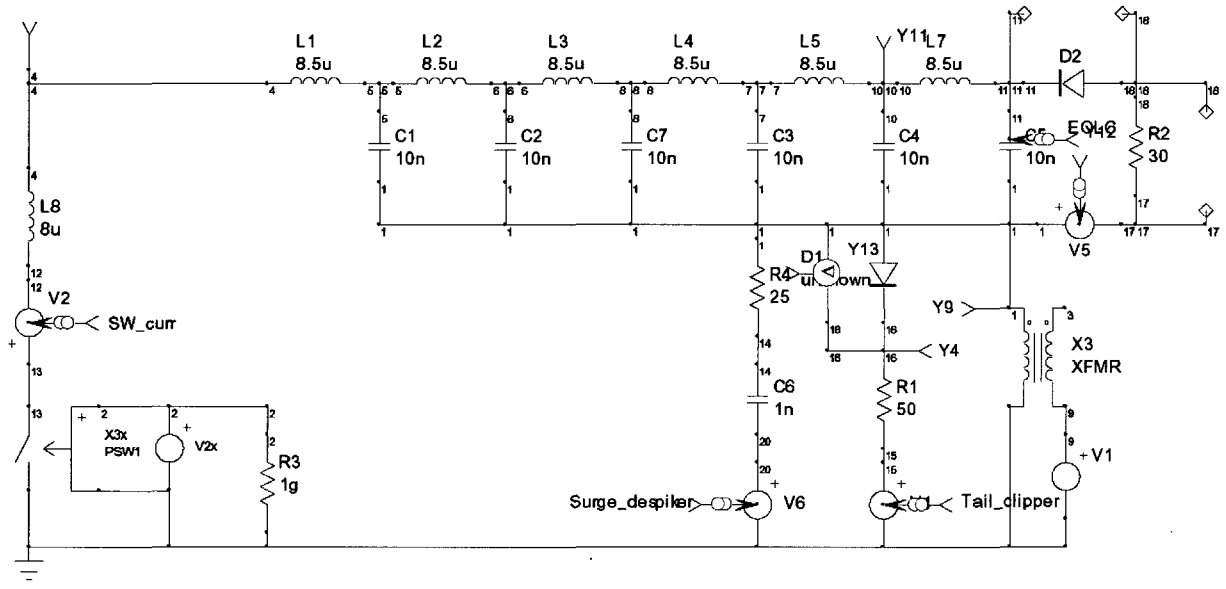


Fig. 8. Simulation Circuit of the Pulsed Modulator System

Fig. 7 shows a set of oscilloscope displays of the final-load voltage and the corresponding current, and the optical trigger waveform obtained in the test circuit of Fig. 4. The peak voltage and current reached 45 kV and 96 A, respectively. The pulse width is 4 μS with a flat-top of 2.8 μS, and the voltage rise time is approximately 0.4 μS with a flatness of 1.8%.

Secondarily, the developed PFN modulator was tested for the magnetron, which has a peak power of 1.5 MW and a pulse duration of 4 μS as the microwave source for the 5-GHz LHCD low-power test system. A 3-dB power splitter in a single waveguide channel was tested with the LHCD low-power test system. In this test, a matching waveguide was shorted and the splitting arms were connected

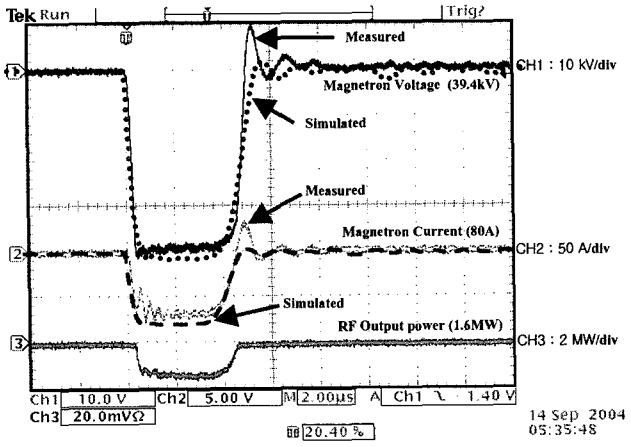


Fig. 9. Tested and Simulated Waveforms for the Magnetron Cathode Voltage, Current and RF Detector Output Voltage

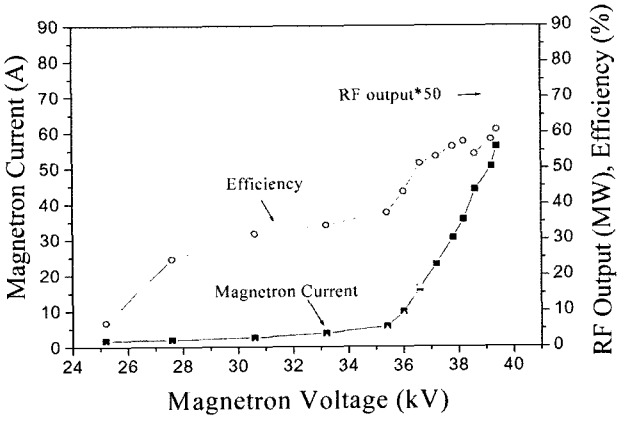


Fig. 10. Characteristics Curve for the 5-GHz Magnetron as a Function of the Magnetron Cathode Voltage

to dry dummy loads. Fig. 8 shows the simulation circuit and parameters of the pulsed modulator system using the IsSpice4 code.

Fig. 9 shows the tested and simulated waveforms for the magnetron cathode voltage, current and RF detector output voltage in two splitting arms. From the measurement of RF power using directional couplers, 665 kW of input power was split into 338 kW for the primary arm and 323 kW for the secondary arm. The power difference between the two arms is merely 2.3 %. The insertion loss in the 3-dB power splitter is 4 kW.

Fig. 10 shows the measured characteristics curve for the magnetron of the current, RF output power, and efficiency as a function of the magnetron cathode voltage.

## 5. CONCLUSIONS

Typically, a modulator system is widely used in pulsed power application systems such as a linear accelerator system, a radar system, a laser system, or an environmental system for the removal of $SO_x$ or $NO_x$. A prototype PFN modulator that operates a 5-GHz, 1.5-MW magnetron was designed and developed. In addition, a pulse transformer with a 1:4 turn ratio was developed to drive a 1.5-MW magnetron for a LHCD low-power test system. The assembled pulse modulator system was studied through a parameter analysis and tested at a high-voltage for a 472 Ω resistive and the 1.5 MW peak power magnetron load on a 5-GHz LHCD low-power test system. In addition, the characteristics test results of the pulse transformer were compared with those of a simulated circuit, and the both results were found to be in agreement. During the development work, a design procedure and formulas were developed. Finally, a test method was set up the for pulse characteristics measurements.

## ACKNOWLEDGEMENT

This work is partially supported by KBSI and the KSTAR project of the Korea Ministry of Science and Technology (MOST). The authors would like to thank POSCON and Don-A Tech. for their assistance with the construction of the pulsed modulator.

## REFERENCES

[1] G. S. Lee et al., "Design and Construction of the KSTAR Tokamak," Nuclear Fusion 41, 1515 ( 2001).

[2] Y. S. Bae, C. H. Paek, M. J. Rhee, W. Namkung, M. H. Cho, S. Bernabei, H. Park, "Design of 5.0-GHz KSTAR Lower-Hybrid Coupler," Fusion Eng. Design 65, 569 (2003).

[3] Y. S. Bae, Ph.D thesis entitled "Lower-Hybrid Wave Heating and Current Drive for KSTAR Tokamak," Pohang University of Science and Technology (2004).

[4] S. D. Jang, Y. G. Son, J. S. Oh, Y. S. Bae, H. G. Lee, S. I. Moon, M. H. Cho and W. Namkung "High-Power Pulse Transformer for a 1.5-MW Magnetron of KSTAR LHCD Microwave Application," Submitted Paper, J. Korean Phys. Soc. (August 29, 2005).

[5] G N. Glasoe and J. V. Lebacqz et al., "Pulse Generators" New York, McGraw-Hill, Part III, pp. 497-630, 1948.

[6] N. R. Grossner, "Transformers for Electronic Circuits," Butterworths, McGraw-Hill, New York, 1967.

[7] J. S. Oh, M.H. Cho, W. Namkung et al., "Efficiency Analysis of the First 111-MW C-Band Klystron-Modulator for Linear Collider," APAC98, KEK, Tsukuba, Japan, March 23-27, 1998.

[8] M. Akemoto, S. Gold, A. Krasynkh and R. Koontz, "Pulse Transformer R&D for NLC Klystron Pulse Modulator," 11th IEEE International Pulsed Power Conference, Baltimore,

Maryland, USA, June 29 - July 2, 1997.
[9] G. M. SUN, E.H. KIM, K.B. Song, et al., Nuclear Engineering and Technology, Vol. 37, No. 2, 185-190, (April 2002).
[10] S. D. Jang, Y. G. Son, J. S. Oh and M. H. Cho, "Development of High-Power Pulse Transformer for Micropulse Type Electrostatic Precipitator Application," 2001 KAPRA & KPS/DPP Joint Workshop, Cheju University, Cheju, Korea, July 6-7, 2001.
[11] S. D. Jang, Y. G. Son, J. S. Oh and M. H. Cho, J. Korean Phys. Soc. 44, 5, 1157 (2004).